A particularly interesting situation occurs for $\frac{1}{2}mv_0^2 \ll \hbar\omega$. Then we find that if $\frac{1}{2}mu^2 \ll \hbar\omega$, the cross section is given by the expression (31) and (31′), with $x \gg 1$. The result is

$$\sigma = \frac{32\pi^2 e^4 q^2 \rho_i}{3\hbar c m^2 \omega^3}(m/2\hbar\omega)^{1/2}\left\{1 - \frac{9}{32}\left(1 - \frac{1}{\sqrt{2}}\right)\frac{e^2E_0^2}{m\hbar\omega^3} + \cdots\right\}, \quad \frac{e^2E_0^2}{m\hbar\omega^3} \ll 1. \quad (43)$$

For $\frac{1}{2}mu^2 \gg \hbar\omega$, we have by Eq. (42)

$$\sigma = \frac{16\pi e^4 q^2 \rho_i \omega}{c(eE_0)^3} \ln\left(\frac{eE_0}{m\omega v_0}\right) \ln\left(\frac{64 m v_0^3 e E_0}{\hbar^2\omega^3}\right), \quad \frac{e^2E_0^2}{m\hbar\omega^3} \gg 1. \quad (44)$$

It is predicted therefore, that with sufficiently strong radiation fluxes, and with the condition $\frac{1}{2}mv_0^2 \ll \hbar\omega$, the absorption cross section will decrease roughly as the three-halves power of the flux. As the intensity is increased, the frequency dependence goes from inverse seven-halves power to direct proportionality.

PHYSICAL REVIEW VOLUME 136, NUMBER 1B 12 OCTOBER 1964

Experiments on the Average Characteristics of Cascade Showers Produced in Lead by 500- and 1000-MeV Electrons*

ERIC E. BECKLIN† AND JAMES A. EARL
School of Physics, University of Minnesota, Minneapolis, Minnesota
(Received 28 February 1964)

The average number and the energy spectrum of shower electrons present under various thicknesses of lead were obtained with the aid of multiplate and magnetic cloud chambers. The relation between observed track length and incident electron energy was found to be

incident energy (MeV) = (23.6±1.6)×track length (radiation lengths).

The observed number of shower electrons with energy greater than 10 MeV is in good agreement with that predicted by recent Monte Carlo calculations; however, low-energy electrons (not included in the calculations) were found to be a large fraction of those present at large depths. Measured probabilities p_n that exactly n electrons emerge from the lower surface of a 0.75-radiation-length lead plate when one electron is incident from above are given as a function of incident electron energy.

I. INTRODUCTION

THE present experiment was originally undertaken to take advantage of the availability of artificially produced beams of energetic electrons for the limited purpose of "calibrating" balloon-borne cloud chambers that had been used to study cosmic-ray electrons. However, it soon became apparent that some of the results obtained were of sufficient general interest to warrant their presentation in this report.

Although existing experimental and theoretical studies have led to a clear understanding of the nature and major characteristics of cascade showers, detailed knowledge of showers developing in materials of high atomic number is needed because such showers provide a useful tool for determining the identity and energy of the initiating electron or photon. It is generally conceded that analytic shower theories[1] yield a useful and essentially correct representation of shower development in materials of low atomic number, but the analysis of showers in high-Z materials is complicated by the intractability of mathematical expressions for the low-energy cross sections of elementary shower processes and by uncertainties arising from the pronounced effects of multiple scattering on low-energy shower particles. These difficulties have been circumvented to a certain extent by Monte Carlo calculations based on exact expressions for the cross sections,[2–5] but even these calculations yield no information on the number of particles present with energy below an arbitrary low-energy cutoff which must be introduced to limit the extent of the computation. Unfortunately, published experimental data on showers in high-Z materials,[6–11] while extensive, are so disjointed that

* Supported by U. S. Office of Naval Research under contract Nonr-710(19).
† Present address: Department of Physics, California Institute of Technology, Pasadena, California.
[1] Summaries of the results of shower theory appear in: B. Rossi, *High Energy Particles* (Prentice Hall, Inc., New York, 1952); and K. Greisen, *The Extensive Air Showers*, in *Progress in Cosmic Ray Physics* (North-Holland Publishing Company, Amsterdam, 1956), Vol. III, pp. 1–141.
[2] R. R. Wilson, Phys. Rev. **86**, 261 (1952).
[3] D. F. Crawford and H. Messel, Phys. Rev. **128**, 2352 (1962).
[4] H. Messel, A. D. Smirnov, A. A. Varfolomev, D. F. Crawford, and J. H. Butcher, Nucl. Phys. **39**, 1 (1962).
[5] C. D. Zerby and H. S. Moran, J. Appl. Phys. **34**, 2245 (1963).
[6] S. Nassar and W. E. Hazen Phys. Rev. **69**, 298 (1946).
[7] W. Blocker, R. W. Kenney, and W. K. H. Panofsky, Phys. Rev. **79**, 419 (1950).
[8] C. A. D'Andlau, Nuovo Cimento **12**, 859 (1954).
[9] W. E. Hazen, Phys. Rev. **99**, 911 (1955).
[10] H. Lengeler, M. Deutschmann, and W. Tejessy, Nuovo Cimento **28**, 1501 (1963).
[11] R. Kajikawa, J. Phys. Soc. Japan **18**, 1365 (1963).

they are not sufficient either to establish unequivocally that any of the calculations mentioned is a suitable tool for the accurate analysis of shower observations or to serve as an empirical basis for such analysis.

The results given here are based on the analysis of photographs of electron initiated shower events in lead obtained with the aid of magnetic and multiplate cloud chambers during an accelerator exposure. This paper presents multiplate data on the average number of electrons present at various penetration depths, multiplate data on the average electron track length associated with a shower of given energy, and magnetic data on the energy spectra of electrons and photons at various depths. (These spectral results are restricted to an incident electron energy of 1000 MeV.) Also presented are various experimental results on the range of shower particles—an important quantity in the treatment of fluctuation phenomena as well as in the design of apparatus. An analysis of fluctuations and correlations in the development of showers will be presented separately.

No extensive comparison of these results with analytic shower theories will be made. However, comparison with Monte Carlo calculations seems worth while in order to determine the extent of their utility as a guide in the analysis of experimental results. The tables prepared recently by Crawford and Messel[3] and by Messel, Smirnov, Varfolomev, Crawford, and Butcher[4] are particularly appropriate for this purpose because they are extensive and presented in a convenient form. Hereafter, these two related papers will be referred to as MSVCB.

II. THE EXPOSURE: DETAILS OF THE CLOUD CHAMBERS

The cloud chambers, which were balloon flight units, were exposed to 500- and 1000-MeV electrons in the external "parasitic" electron beam at the California Institute of Technology Synchrotron. This beam of positive or negative electrons was obtained by magnetic analysis of electrons from pairs produced in a target irradiated by the primary bremsstrahlung gamma-ray beam. The energy and polarity of electrons in this beam were conveniently varied by adjustment of the current through the analyzing magnet coils. The beam energy calibration, furnished by the synchrotron laboratory staff, was accurate to $\pm 5\%$.

Cloud chamber expansions, which occurred at a rate of about one per minute, were synchronized with accelerator pulses (one per second) in such a way that the tracks of beam associated particles were of excellent quality. The number of incident electrons per picture was controlled by adjusting the primary beam intensity. Although this was an effective method of regulating the average number of electrons per picture, intensity fluctuations at the low levels required were very pronounced; consequently, some pictures were blank while others had so many events that they were unusable.

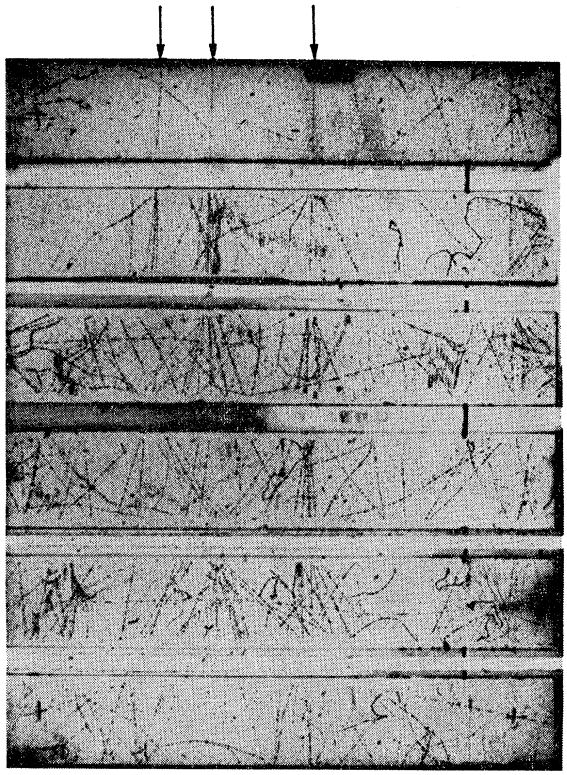

FIG. 1. Three typical 1000-MeV showers as observed in the five-plate cloud chamber.

Two multiplate cloud chambers were used; one had 5 lead plates whose thickness was 1.25 radiation lengths or 7.3 g/cm^2 each, while the other had 9 lead plates of thickness 0.75 radiation length or 4.4 g/cm^2. These chambers were oriented so that the electrons struck the plates at essentially normal incidence. Figure 1 shows a typical 5 plate picture in which showers produced by three incident 1000-MeV electrons are present.

A third cloud chamber, which was operated in a pulsed magnetic field, was used to measure the energy spectrum of shower electrons and photons present under various thicknesses of lead. To determine electron spectra, lead slabs were placed in the incident beam flat against the 1-g/cm^2-thick Lucite front wall of the chamber; then the energies of electrons emerging from the slab were determined from their curvatures as measured by fitting templates to full sized projected images of the pictures. The spectrum of photons emerging from the slab was based on measurements of the energies of electron pairs which some of these photons produced in a single 0.75-radiation-length plate located at the center of the chamber. Figure 2 shows a typical magnetic cloud chamber picture; the configuration of incident beam, lead slab, cloud chamber, and internal lead plate is indicated schematically.

The pulsed magnetic field (2100-G peak and 0.07-sec duration), which was obtained by discharging a large

condenser bank through Helmholtz coils and whose time dependence was that of a highly damped sine wave, was carefully synchronized with the accelerator in such a way that the average field during beam spill-out was 1850 G. Figure 3 shows a resolution function based on magnetic cloud chamber measurements of the apparent energies of 60 electron tracks recorded during an exposure in which electrons of energy 100 MeV (as given by the synchrotron laboratory calibration) were sent directly into the chamber with no external lead slab in place. The excellent agreement between the average apparent energy and the nominal incident energy indicates the correctness of the magnetic and geometrical measurements involved in calibrating the relationship between observed curvature and energy. The width of the resolution curve ($\pm 25\%$) as well as its general shape reflect time variations of the pulsed field during spill out. Dispersion due to errors in the curvature determinations and due to spurious curvature arising from convective track distortion was of relatively minor importance at 100 MeV, but other tests indicated that the "maximum detectable momentum" defined by these effects was about 600 MeV. The resolution in energy outlined above is adequate for the present purposes.

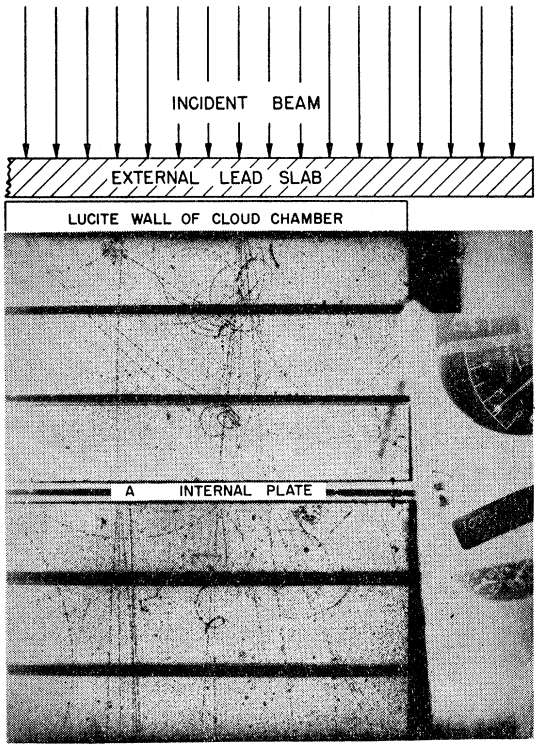

FIG. 2. Curved tracks of shower electrons as observed in the magnetic cloud chamber. Note the narrow angle pair emerging from the internal plate at point A. The four horizontal black bars above and below the plate are clearing field electrodes which are outside the illuminated volume of the chamber. The meter at right indicates pulsed magnet current.

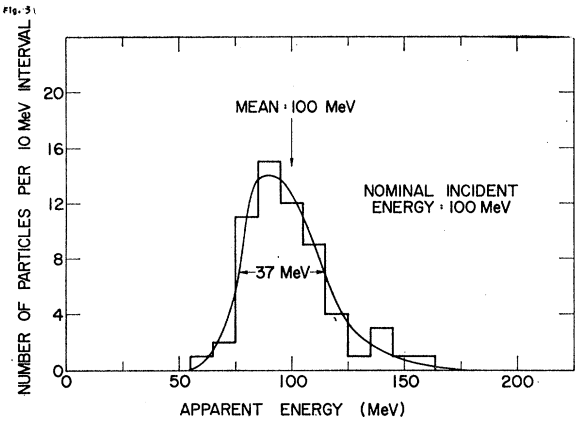

FIG. 3. Empirical resolution function for the magnetic cloud chamber.

III. ANALYSIS OF THE MULTIPLATE DATA: AVERAGE SHOWER DEVELOPMENT

Two distinct procedures, which will be denoted by the adjectives *individual* and *collective*, were used in reducing the data obtained from multiplate pictures such as that in Fig. 1.

In the individual mode of analysis, only track segments which were unambiguously associated with a particular incident electron were counted. Stringent geometrical criteria were imposed on the axes of showers accepted for this type of analysis to ensure that they were well separated from other events and that they were well within the illuminated region of the cloud chamber. The measurements on incident electrons which determined whether or not they satisfied these geometric criteria were done with all sections of the chamber except the first covered. Thus, there was no bias in favor of the selection of large or particularly well-defined shower events. Incident electrons whose directions as observed in the stereoscopic pictures deviated by more than 2 deg from the beam direction were rejected because they may have been scattered from the shielding or from the magnet pole pieces; however, the number of such electrons was negligible. For each acceptable axis, the number of shower associated track segments in each gap between plates was counted and tabulated. Only those track segments which emerged from the plates in the same direction as the incident electrons and within 1 cm of the shower axis were included. In the early stages of shower development, this procedure introduces little or no error because the shower core is very well defined; but, in the later stages where the core becomes diffuse, a small but perceptible number of segments are not counted because they fall outside this 1-cm limit. This point will receive further discussion in a comparison of individual and collective results which comes later. The number of stray background tracks was small enough so that the probability of counting them as shower associated track segments was negligible.

TABLE 1. Multiplate data.

Depth in radiation lengths	Type of chamber	500 MeV Collective			500 MeV Individual			500 MeV MSVCB	1000 MeV Collective			1000 MeV Individual			1000 MeV MSVCB
		Number of showers	Number of particles[a]	Number of particles per shower[b]	Number of showers	Number of particles	Number of particles per shower	Number of particles per shower	Number of showers	Number of particles	Number of particles per shower[b]	Number of showers	Number of particles	Number of particles per shower	Number of particles per shower
0.75	(9)	157	349	1.6±0.1	8	13	1.6±0.5	1.5	178	497	2.0±0.1	34	55	1.6±0.2	1.8
1.25	(5)	210	592	2.3±0.1	15	45	3.0±0.4	2.0	147	656	3.5±0.2	42	143	3.4±0.3	2.6
1.51	(9)	157	474	2.4±0.1	8	22	2.8±0.6	2.2	178	807	3.8±0.1	34	118	3.5±0.3	3.1
2.26	(9)	157	586	3.1±0.15	8	38	4.8±0.8	2.5	178	1081	5.3±0.2	34	151	4.4±0.4	4.1
2.51	(5)	210	766	3.1±0.1	15	48	3.2±0.4	2.5	147	927	5.4±0.2	42	212	5.2±0.4	4.3
3.02	(9)	157	590	3.1±0.15	8	39	4.8±0.8	2.4	178	1224	6.1±0.2	34	179	5.3±0.4	4.6
3.76	(5)	210	715	2.9±0.1	15	35	2.3±0.4	2.1	147	1014	6.0±0.2	42	263	6.3±0.4	4.3
3.78	(9)	157	589	3.1±0.15	8	19	2.4±0.5	2.1	178	1218	6.1±0.2	34	198	5.8±0.4	4.2
4.54	(9)	157	528	2.7±0.15	8	16	2.0±0.5	1.7	178	1229	6.1±0.2	34	193	5.8±0.4	3.8
5.02	(5)	210	568	2.2±0.1	15	19	1.3±0.3	1.4	147	875	5.0±0.2	42	210	4.9±0.4	3.5
5.30	(9)	157	453	2.2±0.1	8	21	2.6±0.5	1.2	178	1057	5.2±0.2	34	157	4.7±0.4	3.1
6.05	(9)	157	367	1.7±0.1	8	10	1.2±0.5	0.9	178	936	4.5±0.2	34	111	3.3±0.3	2.5
6.27	(5)	210	415	1.7±0.1	15	23	1.5±0.3	0.9	147	696	4.1±0.2	42	139	3.3±0.3	2.3
6.80	(9)	157	233	1.1±0.1	8	8	1.0±0.5	0.7	178	598	3.0±0.2	34	85	2.5±0.3	2.0

[a] Total number observed before background correction.

[b] Background subtracted.

In the collective mode of analysis, pictures which had many showers—five to fifteen—were used. All track segments observed in each section were counted irrespective of their association with incident electrons. Incident electrons, which were readily recognizable, were also counted so that the average number of shower tracks in each section per incident electron could be obtained. The validity of this procedure for obtaining the average shower development depends on the absence of edge effects at the boundaries of the sample volume defined by the cloud chamber illumination. Since the lead plates extended well beyond the edges of this illuminated volume and since the electron beam was distributed over an area much larger than the cloud chamber, the results obtained should be a good approximation to those expected for a planar geometry of infinite lateral extent. The collective data were corrected for a small background of stray truck segments consisting of (2.5±0.5) particles per section per picture due to cosmic rays and local radioactivity plus a component due to radiation scattered from the walls of the building which depended on synchrotron intensity and amounted to (0.5±0.2) particles per section per incident electron.

The data obtained from multiplate cloud chamber pictures are presented in Table I and graphed in Fig. 4. Plotted in the figure for 500- and 1000-MeV incident electrons are average shower development curves (i.e., graphs of the mean number of particles present as a function of shower penetration depth t in radiation lengths). Dotted, dashed, and solid lines represent, respectively, the collective data, the individual data and the calculations of MSVBC for electrons of energy greater than 10 MeV. A complete presentation of track length data appears later (Table III), but to simplify intercomparison of the curves in Fig. 4, Table II gives percentage differences from the collective results for the mean number of particles present over the depth interval 0 to 7 radiation lengths.

The following conclusions are based on results presented in Tables I and II and Fig. 4.

(1) The thickness and spacing of the plates have negligible effect on the empirical shower development curves. This is indicated by the lack of any perceptible systematic difference between the five and nine plate data points presented in Fig. 4. Of course, this result is not surprising but, in connection with the problem of estimating energies from multiplate pictures of showers, it is comforting to have empirical verification that the final results are nearly independent of the specific configuration of plates used.

(2) The agreement between the two modes of analysis is very good but there is a small systematic excess of collective over individual which is most apparent in the data of relatively high statistical accuracy taken at 1000 MeV and which averages (8±4)% according to Table II. This deviation may be attributed to those

tracks present in showers which were not counted in the individual analysis because they could not be positively associated with an incident electron. This interpretation also explains why the difference appears larger (in Fig. 4) at great depths where the relatively diffuse structure of showers makes positive association more difficult. Since backscattered tracks were counted in the collective analysis but not in the individual, the figure of (8±4)% also represents an upper limit on the average fraction of backscattered tracks in the depth interval considered.

In spite of this small discrepancy, the over-all consistency of results from the two methods is remarkable. It suggests that the structure of showers is sufficiently well defined so that the procedure used in the individual mode yields an essentially valid representation of the true shower development which may be compared with results independent of lateral structure such as theoretical calculations, ionization measurements or, perhaps, spark chamber measurements.

TABLE II. Comparison of shower development curves.

	500 MeV	1000 MeV
Average number of track segments present (0 to 7 r.l.):		
Collective	2.30±0.1	4.45+0.1
Individual	···	4.10±0.15
MSVCB (E>10 MeV)	1.95	3.61
Percent differences:		
Collective–Individual / Collective	···	8±4
Collective–MSVCB / Collective	15±4	19±3

(3) There are systematic departures of the experimental data from the calculations of MSVCB. These average about 15 to 20% (see Table II) but, in Fig. 4, it appears that the agreement is considerably better than this in the early stages of shower development and considerably worse in later stages. Thus, the calculations, while giving a reasonably accurate account of the early development, predict an earlier maximum and fewer particles at maximum than are observed. On the basis of spectral measurements to be presented in Sec. V, it appears that this discrepancy is due not to a basic flaw in the calculations but to the presence of electrons of energy below 10 MeV which are numerous at and just past the maximum and which are not included in the calculated curves.

The fact that a large fraction of the electrons present at shower maximum have energies below 10 MeV is not surprising. It is suggested not only by analytical calculations of the electron spectrum[12,13] but also by the work of MSVCB in which some of the large number of electrons with energy below 10 MeV considered to be lost to the shower must, in fact, be present. This argument is pursued in more detail in Fig. 5 which compares three curves based on the MSVCB calculations for 1000-MeV showers (solid curves) with experimental results (dotted curve). Curve 1 gives the calculated number of electrons present with energy greater than 10 MeV; curve 2 gives the number per radiation length which drop below 10 MeV and are considered lost; curve 3 gives the number of electrons above 10 MeV plus 26% of the number "lost" per radiation length. The almost perfect coincidence between curve 3 and the dotted curve 4 which represents collective experimental data for 1000 MeV suggests that the mean range of the "lost" electrons (average energy of 7 MeV according to the calculations) is 0.26±0.03 radiation length. Implicit in the procedure used to obtain this range estimate is the assumption that further production of electrons by photons or electrons below 10 MeV is negligible. This

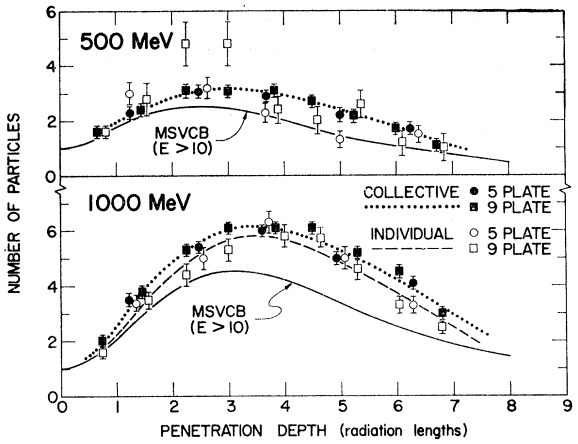

FIG. 4. Average development curves for 500- and 1000-MeV showers.

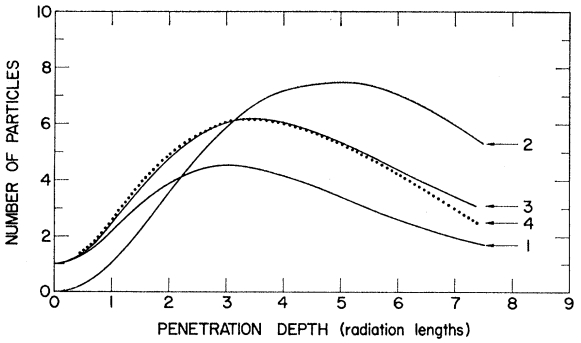

FIG. 5. Comparison at 1000 MeV of curves calculated by MSVCB (solid) and collective data (dotted). See text for detailed explanation.

[12] J. A. Richards and L. W. Nordheim Phys. Rev. 74, 1106 (1948).
[13] I. Tamm and S. Belenky, Phys. Rev. **70**, 660 (1946).

assumption seems justified first because the relevant cross sections are small, and, second, because the calculated mean energy of photons below 10 MeV is only about 1 MeV. Although the nominal range of 7-MeV electrons is about one radiation length, the above result seems plausible in view of the probable large effects of scattering on the apparent range of low-energy electrons.

In spite of the above reconciliation of calculations with experimental results and in spite of the excellent agreement at high energies to be presented later, it would appear that, in real showers developing in materials of high atomic number, the presence of low-energy electrons is a decisive factor which severely restricts the application of calculations involving an arbitrary low-energy cutoff to the important experimental problem of relating the energy of incident electrons or photons to the characteristics of their showers as observed by track forming detectors of limited energy resolution.

IV. TRACK LENGTHS

In this paper, track length is defined as area under the shower development curve and is expressed in radiation lengths (r.l.). This definition gives projected track length; i.e., the contribution of a particle diverging from the shower axis is given by the component of its displacement parallel to the axis.

It is convenient to express the relationship between incident energy and track length in terms of a quantity ϵ defined as the ratio of these quantities. Table III presents track lengths obtained by numerical integration of the experimental shower curves of Fig. 4 and the derived values of ϵ; it also presents these quantities as measured by other investigators and as calculated by MSVCB for shower electrons with $E>10$ MeV. In computing track lengths, an exponential extrapolation function based on a least-squares fit to observations in the depth range from 4 to 7 radiation lengths was used to cover the depth region beyond 7 radiation lengths where there were no data. The logarithmic slope $(-\mathrm{d}\ln n/\mathrm{d}t)$ of this function is given in the column of Table III headed "slope"; for comparison, several other determinations of the shower absorption coefficient at large depths are also presented in this column. Although the values of the track length beyond 7 radiation lengths obtained by the above method are not very precise, the uncertainty associated with the procedure is fairly small because the area under the extrapolation is only a small fraction of the total area. (This can be seen in Table III by comparing the track lengths integrated to 7 radiation lengths with those integrated to infinity.)

TABLE III. Track lengths for showers in lead.

	Depth (r.l.)	Track length (r.l.)	Slope $(\text{r.l.})^{-1}$	ϵ (MeV/r.l.)
Collective 100 MeV	7	31.1±1.5		
	∞	43.7±3.0	0.26±0.06	23.0±2.0
Individual 1000 MeV	7	28.5±1.5		
	∞	35.5±2.5	0.35±0.05	28.2±2.0
Collective 500 MeV	7	16.1±1.5		
	∞	20.2±2.0	0.31±0.06	24.8±2.5
MSVCB ($E<10$ MeV) 1000 MeV	7	25.2		
	∞	31.5	0.34	31.7
MSVCB ($E>10$ MeV) 500 MeV	7	13.7		
	∞	15.7	0.41	31.8
Lengler *et al.*[b] 372,192,92 MeV	∞	...	0.40[a]	23.8±1.4[a]
Hazen[c]	∞	...	...	28[a]
Backenstoss *et al.*[d] 1–10 BeV	∞	...	0.35	10.4
Pugh *et al.*[e] 75, 150, 225 MeV	∞	...	...	10

[a] These values were adjusted to conform with the value of 5.82 g/cm² used for the radiation length in this paper.
[b] H. Lengler, M. Deutschmann, and W. Tejessy, Nuovo Cimento **28**, 1501 (1963).
[c] W. E. Hazen, Phys. Rev. **99**, 911 (1955).
[d] G. Backenstoss, B. D. Hyams, G. Knop, and V. Stierlin, Nucl. Instr. Methods **21**, 155 (1963).
[e] G. E. Pugh, D. H. Frisch, and R. Gomez, Rev. Sci. Instr. **25**, 1124 (1954).

Since there is no statistically significant difference between the values of ϵ for 500- and 1000-MeV showers, it appears that ϵ is independent of incident energy. The excellent agreement between the collective results and the value of ϵ obtained by Lengler *et al.*[10] at relatively low energies is further evidence in favor of this conclusion. Good agreement with a rough estimate of ϵ made by Hazen[9] was also obtained. (This estimate is probably most comparable to the present individual results.) In summary, the value of ϵ obtained from collective data by weighting the 500- and 1000-MeV results according to the numbers of track segments involved was $\epsilon=23.6\pm1.6$ MeV/radiation length.

Although this value of the track length constant is in good agreement with other estimates based on sampling the number of shower particles appearing in gaps in a lead absorber, it is considerably larger than estimates inferred by sampling the ionization in the gaps. (The last two entries in Table III are of this type.) The track length constant expected on the basis of conservation of energy is essentially equal to the critical energy or about 7.5 MeV/r.l.; this value, which, of course, refers to the total rather than the projected track length, is not consistent with that given above but it might be compatible with the ionization determinations. The factor-of-three difference between present results and expected total track length is too large to be dismissed without explanation but its origin is quite obscure. A similar discrepancy of smaller magnitude—a factor of 1.8—was noted in copper by Hazen who interpreted it in terms of a low-energy cutoff below which the ratio of total to projected track length is large because scattering produces a nearly isotropic angular distribution of shower particles. However, it is easy to show that, even for an isotropic distribution of *all* shower particles, the above ratio of track lengths is only two. Since this is significantly less than the observed ratio and since the absence of backscattered tracks indicates a forward

collimation of shower tracks, it appears that some mechanism other than scattering is needed to explain the present observations.

Whatever this mechanism may be, it seems clear that only one-third to one-half of the total shower energy is dissipated as ionization by particles seen in typical multiplate track counting detectors. We suggest that the rest of the shower energy eventually appears as kinetic energy carried by large numbers of nonrelativistic electrons in the 10–300-keV energy range. Such electrons are expected as products of the photoelectric and Compton collisions in which the numerous low-energy photons known to be present in showers dissipate their energy. The presence of these electrons could explain both the present results and the ionization measurements. Because of their low velocity, they would make a large contribution to the ionization, but, because of their short range and isotropic distribution, their contribution to the projected track length would be very small. The fact that the slow electron component would have an isotropic distribution also explains why the upper limit on the fraction of backscattered tracks given earlier was only $(8\pm4)\%$ while Blocker, Kenney, and Panofsky[7] observed that 40% of the ionization was due to backscattered particles.

Although many tracks exhibiting the pronounced gas scattering and relatively heavy ionization characteristic of nonrelativistic electrons were observed in the multiplate pictures (see Fig. 1), a direct evaluation of the track length due to shower associated slow electrons was not possible because of the presence of large numbers of unassociated low-energy electrons arising from scattered synchrotron radiation, local radioactivity, and production of δ rays by fast shower electrons. Nevertheless, it is interesting to estimate the number of shower associated low-energy tracks that would be seen assuming the correctness of the above hypothesis. This can be done as follows for 1000-MeV showers: The total observed track length is 53 radiation lengths which corresponds to a "visible" energy of $53\times7.5=400$ MeV. (The total track length was obtained by multiplying the projected track length given in Table III by a factor of 1.2 ± 0.05 which is the average value of cosecant θ calculated from values of the zenith angle θ of shower tracks measured with the aid of a stereoscopic reprojection system.) Suppose that the "missing" energy (600 MeV) is transferred to twelve thousand 50-keV electrons. Since the projected range in lead of each electron is 3.3×10^{-4} radiation length (this is half of the total range computed from the nonrelativistic formula for energy loss by ionization), the projected track length of all of these electrons would be 4 radiation lengths. Thus, in a chamber having plates of thickness 1.25 radiation lengths (five plate), only three of the twelve thousand electrons would appear; these electrons, which could have any energy between 0 and 50 keV and which might emerge on either side of the plates, would be almost impossible to separate from the background.

A specific energy of 50 keV was used above for purposes of illustration, but the calculation can easily be carried out assuming transfer of 600 MeV to electrons of an arbitrary nonrelativistic energy E; the result is summarized by the equation

$$\text{visible projected low-energy track length} = E(\text{keV})/12.5 \text{ (in radiation lengths)}.$$

The fact that the track length given by this expression must be compatible with observations can be used to set an upper limit on the energy of the electrons assumed to carry the "missing" shower energy. This upper limit is 300 keV; the predicted 24 radiation lengths of track length in electrons of about this energy would be an unmistakable feature of both the multiplate and magnetic pictures but was not observed.

Although the above hypothesis involves the transfer of a surprisingly large amount of energy to slow electrons, the following argument based on the MSVCB calculations indicates that this is not impossible. The calculated percentages of the original shower energy appearing in electrons and photons of energy less than 10 MeV are, respectively, 40.37 and 30.44. Since the average energy of electrons produced by these photons is considerably less than the average photon energy—which is only 0.9 MeV according to the calculations—it seems reasonable to assume that all of the above photon energy eventually is transferred to electrons with $E<300$ keV. (It is to be noted that energy dissipation by photons in the 0.5- to 10-MeV region involves the production of numerous low-energy electrons through the processes of multiple Compton collisions, pair production followed by photoelectric conversion of annihilation quanta, etc.) About half of the energy in electrons with $E<10$ MeV (average calculated energy of 7 MeV) is radiated as photons which will also produce slow electrons. Thus, the percentage of shower energy which is expected to appear in nonrelativistic electrons is roughly $30.44+\frac{1}{2}\times40.37=50.6$—a value close enough to the "observed" value of 60% to suggest the basic validity of the hypothesis.

V. ANALYSIS OF THE MAGNETIC DATA: ENERGY SPECTRA OF ELECTRONS AND PHOTONS

In the analysis of magnetic cloud chamber pictures such as that shown in Fig. 2, only those tracks emerging from the external lead slab within a small area at the center of the illuminated region were used. This geometrical criterion ensured that the illuminated length of accepted tracks was adequate for accurate curvature measurements. For tracks emerging normal to the slab, the illuminated length was 10 cm. Electrons emerging from the internal plate were not used because it was felt that their spectra might be distorted as a result of certain geometrical effects. (The data taken at a depth

of 0.75 radiation length do refer to electrons emerging from the internal plate, but they were obtained under conditions—direct exposure to incident electrons with no slab in place— in which these geometrical effects were absent.) An attempt was made to select only those tracks appearing in recognizable shower events. An uncertainty arose because electrons with energies below 2 MeV were unable to penetrate the Lucite wall of the cloud chamber. Data on the number of such electrons obtained during a short run in which the 5-plate chamber was operated in the magnetic field were used to eliminate this uncertainty. Measured energies of electrons emerging from the slab were corrected for energy lost in the Lucite.

Integral energy spectra of shower electrons present at penetration depths ranging from 0.75 to 5.5 radiation lengths are graphed in Fig. 6 and tabulated in Table IV. All spectra discussed in this paper refer to 1000-MeV incident electrons. The solid curves at each depth represent spectra computed by MSVCB. Three spectra at shower maximum are compared at the bottom of the figure: The dotted curve represents the spectrum predicted by the analytical calculations of Richards and Nordheim,[12] the dashed curve represents the experimental spectrum obtained by Nassar and Hazen[6] and the solid curve represents the spectrum calculated by MSVCB at $t=3.5$ r.l. Table V summarizes some features of the spectra considered in Fig. 6; for each depth it gives median energies and the percentage of electrons with energy below 10 MeV.

Since no information on the number of incident electrons was available from the magnetic pictures, all of the spectra were normalized to 100 at zero energy; so that the experimental quantity presented is the percentage of shower electrons with energy greater than

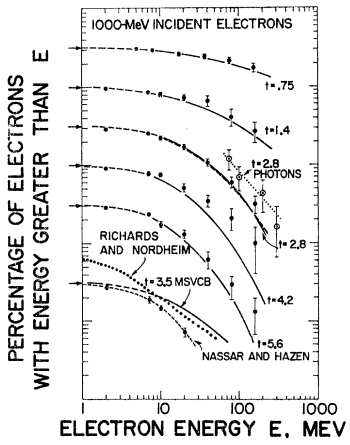

FIG. 6. Observed and calculated energy spectra (also presented in Table IV). The solid lines represent spectra calculated by MSVCB. For clarity, each curve has been displaced vertically by one-half decade from the next, but all the spectra are normalized to 100 at zero energy. Thus, to obtain percentages, the arbitrary logarithmic scale should be moved along the vertical axis until 100 falls at the arrow associated with the curve being considered.

E as a function of E. However, the absolute number of particles above a given energy can readily be obtained by combining the normalized spectral data of Fig. 6 and Table IV with the total number of particles of all energies as given by the collective shower development curve (Fig. 4). For convenience in performing this calculation, the total number $\bar{n}$ is given in Table IV for each depth considered. The normalization of MSVCB results was accomplished by dividing the calculated number of particles above a given energy by the experimental total number of particles above zero energy obtained from the collective analysis. This procedure, which has the effect of extending the calculations below their original minimum energy of 10 MeV, yields a

TABLE IV. Spectra of electrons and photons in 1000-MeV showers.

Percentage of particles with energy $>E$

Electrons

E (MeV)	$t=1.4$	$t=2.8$	$t=4.2$	$t=5.6$
2	95± 2	92±2	92±2	92±2
7	85± 4	81±4	78±4	76±4
10	80± 5	71±4	75±4	56±5
20	73± 6	54±4	51±6	42±5
40	66±10	34±4	35±6	20±6
80	41±10	19±3	21±7	9±4
160	27± 8	10±3	10±6	4±2
Total shower electrons, ($E>7$ MeV)	35	133	40	55
$\bar{n}$	3.7	5.9	5.9	4.7

Electrons ($t=.75$) ($\bar{n}=2.0$)		Photons ($t=2.8$)	
E (MeV)	Percent	E (MeV)	Percent[a]
5	97±2	75	38±11
8	93±3	100	22± 8
17	84±5	200	14± 6
37	77±6	300	5± 3
77	68±6		
154	55±7		
Incident electrons	39		
Total shower electrons	62		

[a] The photon spectrum is expressed in terms of the ratio of the number of photons with energy greater than E to the total number of electrons present.

"calculated" curve based on data completely independent of that used in constructing the experimental spectra. Thus, although normalization was involved, the "calculated" curves can be compared with the data points on an essentially absolute basis.

Direct normalization of the Richards and Nordheim spectrum to experimental data at zero energy leads to inconsistencies arising from the discrepancy between observed and expected total track length which was discussed earlier. Therefore, the curve representing this spectrum in Fig. 6 was displaced upward in such a way as to give the correct ratio of total to observed track length above zero energy. (This ratio is 3.15.)

An estimate of the effect of the finite energy resolution

was obtained by numerically folding the resolution function of Fig. 3 into a typical MSVCB spectrum. The resulting curve, which would represent the experimental results if the true spectrum were exactly that of MSVCB, is shown as a dashed curve associated with the data at $t=2.8$ radiation lengths. It is clear that, at this depth and by implication at all depths considered, spectral distortions arising from the finite resolution in energy are small compared to statistical uncertainties.

The results presented in Fig. 6, Tables IV and V lead to the following conclusions:

(1) The spectrum of shower electrons is strongly dependent on penetration depth. At small depths, the curves are essentially a reflection of the bremsstrahlung energy loss of incident electrons, while at large depths, where multiplication and absorption processes are dominant, the slope of the spectral curves increases rapidly with increasing depth. Although the curves are not congruent when presented as log-log plots and, consequently, cannot be expressed in terms of a single depth-dependent energy parameter, the fact that the median energy decreases as $t^{-1.0\pm0.2}$ provides a useful approximate description of this depth variation. This representation may or may not be valid at greater depths than observed, but, in any case, the progressive softening of the spectrum apparent in Fig. 6 seems to be a well-established trend which might be expected to continue at greater depths than those considered. The qualitative nature of this depth dependence is very similar to the softening with increasing shower age predicted by analytic theories. However, the application of such theories to the present experiment is so questionable that a more detailed comparison seems inappropriate.

(2) Within the limitations imposed by statistics and by the probable existence of a residual geometric bias against low-energy particles which tends to make high-energy experimental values too large, the solid MSVCB curves are a good representation of the measured spectra. At $t=2.8$ radiation lengths, where experimental points of relatively high statistical accuracy were obtained, the agreement is particularly good. Thus, the present comparison confirms the accuracy of the MSVCB calculations within the energy range claimed for their validity. However, it must be pointed out that this range begins at 10 MeV and that the observed excellent agreement was obtained through the use of a normalization procedure which, in essence, introduced experimental results as a supplement to the calculations in the crucial energy range from 0 to 10 MeV. The last two columns of Table V show data which indicate the importance of electrons with energies in this range and which confirm the assertion made earlier that the presence of such electrons can account for the observed differences between calculations and collective results. Both columns present estimates of the percentage of all shower electrons with energy below 10 MeV as a function of penetration depth; the estimate headed "From Spectral Data" is based on the magnetic data of Table IV and Fig. 6, while that headed "Inferred from Shower Curves" is simply the percentage difference between MSVCB calculations and the collective results. It is evident that these estimates are consistent and that, at large depths, up to 45% of the shower electrons are observed to have energies below 10 MeV.

TABLE V. Summary of spectral results.

Depth in radiation lengths	Median energies (MeV)		Percentage of electrons with $E<10$ MeV	
	MSVCB	Present experiment	From spectral experiment	Inferred from shower curves
0.75	150	210±50	10±4	10
1.4	41	60±30	20±5	24
2.8	22	24±3	29±4	24
4.2	16	22± 6	25±5	30
5.6	12.5	15± 5	44±6	40

(3) At energies above 10 MeV, the normalization described earlier brings the track length spectrum calculated by Richards and Nordheim into good agreement with experimental results. (These are well represented at shower maximum by the MSVCB curve for $t=3.5$ r.l.) This agreement is evidence for the validity of these calculations in an energy region where the importance of scattering and other effects which tend to make the observed spectrum of emerging electrons different from the calculated spectrum of electrons within the lead is minor. The absence of the relatively large numbers of low-energy electrons predicted by the calculations indicates, perhaps, that the mechanism responsible for the track length discrepancy discussed earlier operates mainly upon low-energy electrons, but, other than this, it throws little additional light on the nature of this mechanism.

(4) The spectrum measured by Nassar and Hazen at shower maximum is qualitatively similar to the present spectra but it is somewhat steeper than the spectrum at maximum inferred from present results. Since the dependence of spectral shape on depth is strong and since some dependence on initial energy is probable, this discrepancy is not surprising in view of the fact that the cosmic-ray source used in the earlier experiment did not lend itself to exact specification of these variables.

The photon spectrum. The spectrum of photons at shower maximum (shown in Fig. 6 as open circles and a dotted line associated with the results obtained at $t=2.8$ radiation lengths) was obtained from estimates of the number of pairs produced in the 0.75-radiation-length plate at the center of the magnetic chamber by photons emerging from the external slab (see Fig. 2). Events in which two associated electrons of opposite sign emerged from this plate were assumed to be pairs

and the photon energy was assumed to be the sum of the two electron energies. On the grounds that a knock-on electron should occasionally be associated with one of the members of the pair, a few triplets were also interpreted as photon events; the number of such cases was consistent with measured knock-on probabilities to be presented shortly. Singly emergent electrons, some of which were undoubtedly Compton electrons or surviving electrons from pairs whose other member stopped in the plate, were observed but not included in the data used to construct the photon spectrum. The directions of the electrons in accepted photon events were required to be such that, with an appropriate allowance for scattering, the photon could have originated in a recognizable shower developing in the external slab.

A complicated calculation involving the angular distribution of shower electrons and photons and the geometry of the apparatus was avoided by normalizing the number of photons observed at each energy to the number of shower electrons which penetrated the plate and whose paths below the plate satisfied the same geometric criteria used to select acceptable photon events. If the angular distributions of emergent electrons and photons of a given energy are identical, this procedure yields rigorously correct results; but, in any case, the fact that the high-energy electrons and photons considered are quite strongly collimated in the direction of the incident beam suggests that errors associated with this admittedly imprecise method of dealing with the geometry are small compared to statistical uncertainties.

The number of emergent photons was calculated from the observed number of pair events through the use of well-known theoretical results for the probability of pair production in lead and an empirical estimate for the probability that both pair electrons escape from the plate. The data on which this empirical estimate was based have some intrinsic interest and will be presented shortly; but, in the present context, the main result obtained was that only the lowest energy point on the photon spectrum of Fig. 6 was significantly dependent upon the estimated value of the pair escape probability. It seems that there is a "cutoff" energy below which true pairs are not to be expected and above which the escape probability is large and relatively independent of energy. In the present experiment, this "cutoff" occurred at about $E_{\text{pair}}=50$ MeV; for the lowest energy point of Fig. 6—$E_{\text{pair}}=75$ to 100 MeV—the probability was about 0.5; while, for higher energies, it ranged from 0.75 to 0.9 and was fairly independent of energy and of the effective thickness which it was assumed that all the pair electrons had to penetrate in order to escape. Thus, the form of the experimental photon spectrum is not subject to large errors arising from uncertainties in the escape probability.

In the energy range from 75 to 300 MeV, the experimental photon spectrum at $t=2.8$ radiation lengths has about the same slope as the electron spectrum, but the absolute number of photons above a given energy is 1.7 ± 0.3 times as great as the number of electrons. This result is consistent with a value of 1.3 which is the ratio predicted as a high-energy limit by analytic theories. Although MSVCB do not present explicit photon spectra, their calculations of the total energy carried by photons of energy greater than 10 MeV are consistent with the above ratio and with the observed absolute number of photons provided that the spectrum of photons above 10 MeV is assumed to be identical in slope to that calculated for electrons. Thus, it appears that, in the high-energy range, the observed photon spectrum is in good accord with calculations but that further experimental work is needed to define the photon spectrum below 75 MeV.

VI. ELECTRON PENETRATION PROBABILITIES IN LEAD

Figure 7 presents the data used to estimate pair escape probabilities which, as was mentioned earlier, are of some interest because they refer to penetration of high-Z absorbers by high-energy electrons—a domain which, to the knowledge of the present authors, has not been adequately explored. Plotted here as a function of incident electron energy E are n-fold "penetration probabilities" for the 0.75-radiation-length lead plate of the magnetic cloud chamber. These are the probabilities p_n that exactly n electrons emerge from the lower surface of the plate when one electron of energy E is incident from above. For energies below 100 MeV, the data are based on observations of shower electrons emerging from the slab whose energies were obtained from curvature measurements while, for energies above 100 MeV, the data are based on observations of directly incident electrons whose energies were given by the synchrotron calibration. Although these penetration curves refer to only one thickness and are not very precise, they may, at least, be useful in guiding the design of apparatus; furthermore, they have some qualitative features which, if confirmed by observations at other thicknesses, might be used to analyze electron spectra at fairly high energies just as the results of exhaustive earlier studies of absorption in low-Z ma-

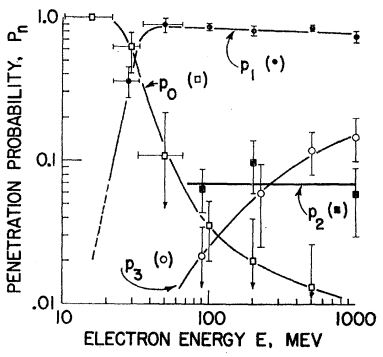

FIG. 7. Penetration probabilities for a 0.75-radiation-length lead plate. p_n is the probability that exactly n electrons emerge from the plate when one electron of energy E is incident.

terials have been extensively applied in the analysis of beta decay spectra.[14]

For each value of n considered in Fig. 7, the curve of p_n versus E can be interpreted in terms of the most probable process leading to the emergence of n electrons. For $n=3$, this process is bremsstrahlung followed by escape of both members of a pair produced within the plate by the emitted gamma ray. That this is actually the case is suggested, first, by the almost total absence of events in which more than three electrons emerged and, second, by the observed variation of p_3 with energy which seems to reflect the fact that, as their average energy decreases, the probability that all three electrons escape from the plate also decreases. Knock-on collisions are suggested as the main process leading to emission of two electrons by the facts that p_2 is nearly independent of energy and that its magnitude is consistent with the value of 0.07 secondary electron per particle which is commonly quoted as the average number of knock-on electrons emerging from lead in association with cosmic-ray mesons.[15,16]

The quantities p_1 and p_0 are, respectively, the probabilities of simple penetration (perhaps with considerable scattering and energy loss) and simple absorption. These processes are, of course, dominant since p_2 and p_3 are small quantities describing relatively improbable events. The main feature of the curves for p_1 and p_0 is an abrupt transition from complete absorption to nearly complete penetration within a narrow energy interval centered at about 30 MeV. Although the position and sharpness of this cutoff are presumably determined by a complicated combination of effects due to scattering, energy loss by ionization and radiation, and, at high energies, cascade multiplication, it might be expected to be reasonably sharp for energies above those for which isotropic diffusion due to scattering is dominant (about 10 MeV) and below those for which cascade multiplication is dominant (about 200 MeV). Thus, on the basis of present results, it seems that penetration measurements might be a useful tool for estimating electron energies within this range.

Since the pair electrons considered earlier in connection with the photon spectrum were produced throughout the plate, a rigorous computation of the pair escape probability would require penetration data not only for the full thickness of the plate, but also for smaller thicknesses. In the absence of such data, it was assumed that the absorption probability p_0 for pair electrons produced in the plate was given by a curve of the same shape as that for p_0 in Fig. 7 but shifted to the left by a factor of 2. Although this assumption would be strictly valid only if the "range" defined by the sharp cutoff were proportional to electron energy, its use here seems justified even in the absence of evidence for such an energy dependence because the measured photon spectrum does not depend sensitively upon details of the pair escape calculation.

VIII. SUMMARY

The most important results presented above are:

(1) The track length constant ϵ was found to be

$$\epsilon = 23.6 \pm 1.6 \text{ MeV/radiation length}.$$

(2) Although good agreement with the MSVCB calculations was obtained at energies above 10 MeV in spectral experiments, the presence of large numbers of electrons below this energy was found to be a factor which seriously limits the usefulness of these calculations in analyzing experimental observations of real showers.

ACKNOWLEDGMENTS

The authors would like to thank Professor Robert L. Walker and Professor Alvin V. Tollestrup, the graduate students, and the staff of the California Institute of Technology Synchrotron Laboratory for the hospitality and cooperation which made the exposure possible. Thanks are due to Professor H. Messel for making available before publication the results of his group's Monte Carlo calculations. James Sarp deserves special credit for preparing the equipment for shipment and for assisting during the accelerator run.

[14] L. Katz and A. S. Penfold, Rev. Mod. Phys. **24**, 28 (1952).
[15] W. E. Hazen, Phys. Rev. **64**, 7 (1943).
[16] W. W. Brown, A. S. McKay, and E. D. Palmatier, Phys. Rev. **76**, 506 (1949).

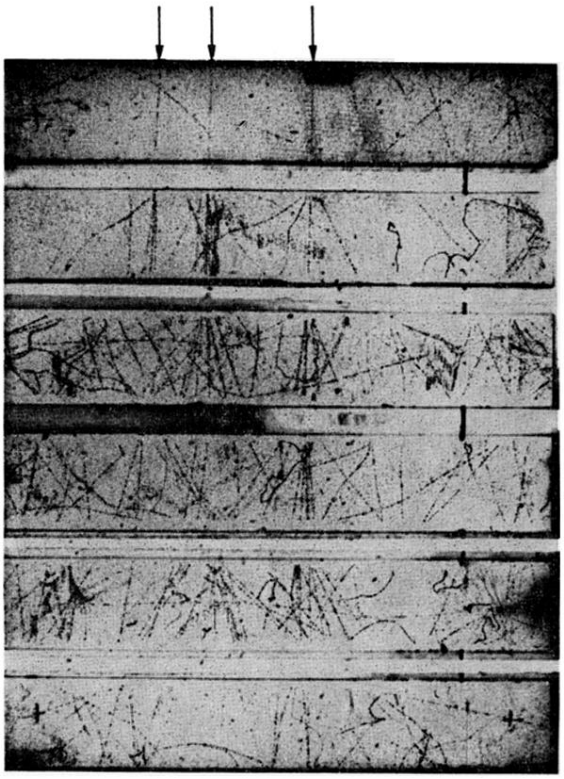

FIG. 1. Three typical 1000-MeV showers as observed in the five-plate cloud chamber.

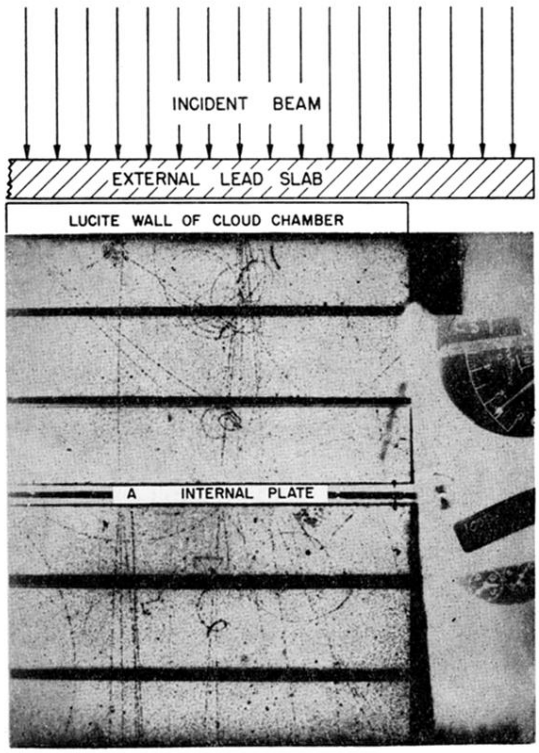

FIG. 2. Curved tracks of shower electrons as observed in the magnetic cloud chamber. Note the narrow angle pair emerging from the internal plate at point A. The four horizontal black bars above and below the plate are clearing field electrodes which are outside the illuminated volume of the chamber. The meter at right indicates pulsed magnet current.